ORIGINAL ARTICLE

CrossMark

Characterization of alkali-extracted wood by FTIR-ATR spectroscopy

Joni Lehto[1] · Jarmo Louhelainen[1] · Teresa Kłosińska[2] · Michał Drożdżek[2] · Raimo Alén[1]

Abstract
Attenuated total reflectance (ATR) infrared (IR) spectroscopy analyses were performed with silver/white birch (*Betula pendula*/ *B. pubescens*) and Scots pine (*Pinus sylvestris*) chips pretreated under alkaline (from 1 to 8% NaOH charge on wood dry solids) conditions to determine the suitability of this method in quickly determining chemical changes caused by varying treatment conditions on wood chemical structure. In addition to the alkali charge, pretreatment conditions varied with respect to temperature (130 and 150 °C) and treatment time (from 30 to 120 min). The spectral data of pretreated wood samples were compared to those of untreated reference samples, and the effects of the pretreatments conducted were determined based on these data. Results indicated that the most essential phenomena taking place during alkaline pretreatments could be detected by applying this simple and rapid spectral method requiring only a small sample amount. Such information included, for example, the cleavage of common lignin and carbohydrate bonds together with the significant removal of organics, especially hemicelluloses during pretreatments.

Keywords Alkaline pretreatment · ATR spectroscopy · Characterization · Infrared · Wood

1 Introduction

A stepwise conversion of the present, global, fossil-resource-based economy into a sustainable bio-based one (i.e., primarily using bioenergy, biochemicals, and biomaterials) has recently been considered to be one of the most important shifts in society [1–4]. Although a wide variety of raw materials and sources (wind, sun, hydro, and biomass resources) can be utilized for the production of energy, the industry sector producing materials depends mainly on plant biomass. This transformation has promoted the evolution of novel biorefineries utilizing different renewable raw materials, such as those from agriculture (dedicated crops and residues), forestry, industry, household (process residues, leftovers, municipal solid waste, and wastewater), and aquaculture (algae and seaweeds) for producing chemicals and materials previously manufactured

mainly from fossil resources [5–7]. Within this scope, biorefineries integrated into forest industry operations and facilities have proven to be one of the most promising alternatives in the production of materials, chemicals, and energy from lignocellulosic materials.

The integrated forest biorefinery (IFBR) concept consists of the addition of biorefining units to existing pulp and paper mills while maintaining the manufacturing of their core product (i.e., cellulosic fiber) [7–10]. The IFBR approach has significant economic advantages over autonomous biorefineries, as pulp mills can offer the infrastructure (i.e., utilities, laboratories, and wood handling), supporting networks (i.e., material and chemical suppliers and markets for products), direct access to raw materials, attractive utility costs (i.e., steam and water), and qualified human resources [7, 10–12]. In modern IFBRies, the main aim is to maximize the value of the used feedstocks by introducing new process alternatives and manufacture of novel product applications besides cellulosic pulp, thus widening the product portfolio of the mills.

One of the most studied IFBR techniques is based on the different pretreatment processes by which wood chips can be partially solubilized under varying conditions (pH, temperature, and treatment time) prior to the actual delignification. These processes produce carbohydrates- and lignin-containing hydrolysates, which can be further converted into desired chemicals, biomaterials, or biofuels [13–16]. Of the

✉ Joni Lehto
joni.t.lehto@jyu.fi

1 Department of Chemistry, Laboratory of Applied Chemistry, University of Jyväskylä, P.O. Box 35, 40014 Jyväskylä, Finland

2 Department of Wood Science and Wood Preservation, Faculty of Wood Technology, Warsaw University of Life Sciences - SGGW, 159 Nowoursynowska St, 02-776 Warsaw, Poland

many possible chemical pretreatments, particularly the pre-treatments conducted under alkaline conditions have been considered a promising and well-integrated biorefinery process combined with existing industrial alkaline pulping process [17, 18]. These pretreatments can shorten cooking time, lower the need for alkali charge of the subsequent pulping phase, and alkaline liquors, such as green and white liquors, can be used for pretreatments [19–21]. In addition to producing valuable organics-containing effluents, alkaline pretreatment processes also have a profound effect on the wood material and its delignification behavior [22–24]. As a part of the hemicelluloses, acetyl groups, lignin, and extractives are removed during the pretreatments, the morphology and chemical composition of wood are also profoundly changed. Additionally, the reactivity of the treated material toward cooking chemicals increases, leading to enhanced pulping performance and the recovery of potential by-streams (lignin and aliphatic carboxylic acids). However, the effects of pretreatments on wood composition must be known in detail in order to maintain the pulp quality. This target creates a need for rapid analysis methods for determining the composition of wood and for evaluating the changes caused by pretreatments.

Several spectroscopic analysis methods, such as Fourier transform infrared (FTIR) [25–27], near infrared (NIR) [28, 29], and attenuated total reflectance (ATR) [30, 31] spectroscopies, have been utilized to determine the composition of various lignocellulosics-based raw materials before and after various chemical treatments and modifications. The advantages of the abovementioned methods are that the instrumentation is usually low-cost, easy to use, and widely available, and because these methods generally only require very little sample preparation compared to many wet chemistry analyses typically utilized in the wood and cellulosic chemistry.

In this study, alkali-extracted hardwood (silver/white birch) and softwood (Scots pine) chips were investigated by an ATR spectroscopic method. The main aim was to determine the effects of varying pretreatment conditions (i.e., alkali charge, pretreatment time, and temperature) on the wood material.

2 Materials and methods

2.1 Raw materials for pretreatment experiments

Screened (SCAN-CM40:94) [32] industrial silver/white birch (*Betula pendula/B. pubescens*) and Scots pine (*Pinus sylvestris* L.) chips were provided by Metsä Group's Äänekoski Bioproduct mill, and they were used in the alkaline pretreatment experiments. Chips having knots, bark residues, and other visible impurities were manually removed prior to the pretreatments. The maximum thickness of the used chips was 7 mm, maximum width 13 mm, and minimum width 7 mm.

2.2 Pretreatments

Laboratory-scale pretreatment experiments of the chips were conducted in 1.25-L rotating stainless steel autoclaves heated in an oil bath (CRS Autoclave System 420, CRS Reactor Engineering AB, Stenkullen, Sweden). Chips were treated at two temperatures (130 and 150 °C), with four treatment times (30, 60, 90, and 120 min). In each case, a 30-min heating period was added to the treatment times. The chosen cooking liquors were aqueous NaOH solutions having chemical additions adjusted to 1, 2, 3, 4, 6, and 8% of NaOH on oven-dried wood. The liquid-to-wood ratio was adjusted to 5 L/kg. After sufficient treatment time, wood chips were separated from the effluents by using filtration bags (280×300-mm monofilament nylon bags, L.K. Suodatin, Siivikkala, Finland). Chips were washed with tap water, and the yield was calculated based on the dry solids (DS) content of untreated and pretreated chips.

2.3 Chemical analyses

For the chemical analyses, wood samples were ground in a Retsch SM100 (Retsch GmbH, Haan, Germany) cutting laboratory mill equipped with a bottom sieve with trapezoidal holes (perforation size of < 1.0 mm) and stored in plastic bags. Prior to compositional analysis, the moisture content of the samples was determined. All analyses were done in duplicate, and the results reported were calculated as percentages (mean values of duplicate samples) of the original dry wood.

The extractives content of the ground samples was determined by extracting the wood flour with acetone in a Soxhlet apparatus according to TAPPI Test Method T280 pm-99 [33]. The extract obtained was first concentrated by vacuum evaporation with a rotary evaporator (Heidolph VV2000, Gemini BV Laboratory, Apeldoorn, the Netherlands) apparatus, and drying was accomplished before weighing by means of a gentle nitrogen gas stream.

The lignin content of the extractives-free sawdust samples (each about 200 mg) was determined as the sum of "acid-insoluble Klason lignin" and "acid-soluble lignin" according to TAPPI Test Methods T222 om-98 [34] and T250 um-00 [35]. Extracted sawdust was treated with 72% H_2SO_4, and the precipitated lignin was filtered off, washed, dried, and weighed. The content of acid-soluble lignin was determined using a Beckman DU 640 UV/Vis-spectrophotometer (Beckman Instruments Inc., Fullerton, CA, USA) at 205 nm after dilution of one portion of the hydrolysate with H_2SO_4 until the absorbance (*A*) was in the 0.3 to 0.8 range. The concentration of dissolved lignin (*c*, g/L) was calculated according to Eq. 1.

$$c = \frac{A}{a*b} \qquad (1)$$

where a is absorptivity (110 L/(g × cm) for hardwoods and 120 L/(g × cm) for softwoods) [36] and b is the path of light (cm). The content of different monosaccharides (i.e., arabinose, galactose, glucose, mannose, and xylose) in the Klason hydrolysates was determined with a Dionex (Dionex Corp., Sunnyvale, CA, USA) high-performance liquid chromatography equipped with pulsed amperometric detector (HPLC-PAD) method previously described elsewhere [37, 38].

2.4 ATR analyses

The samples for the ATR analyses were ground to fine powder using a Fritsch Pulverisette analytical grinder (Fritsch GmbH, Idar-Oberstein, Germany) equipped with a 0.5-mm sieve. In each case, ATR measurements were made from a pellet pressed from the ground sample with a Bruker Alpha FTIR spectroscopic device (Bruker Corp, Billerica, MA, USA) fitted with a Platinum ATR single reflection diamond ATR module that measured the spectra in the wavenumber range from 400 to 4000 cm^{-1}. In the measurements, 64 scans were obtained, and the spectral resolution used was 4 cm^{-1}.

3 Results and discussion

3.1 Raw materials and pretreatments

The chemical composition of the birch feedstock dry mass used for alkaline pretreatments was as follows: carbohydrates 64.1% (of which arabinose 0.4%, galactose 1.3%, glucose 39.7%, mannose 1.6%, and xylose 21.1%), lignin 22.1% (of which acid-soluble 4.8% and Klason 17.3%), extractives 3.1%, and others 10.7%. For the pine feedstock, the corresponding composition was carbohydrates 60.4% (of which arabinose 1.4%, galactose 1.8%, glucose 39.3%, mannose 13.8%, and xylose 4.1%), lignin 27.7% (of which acid-soluble 0.5% and Klason 27.2%), extractives 3.7%, and others 8.2%. The yields (calculated as % of dry wood) after alkaline pretreatments were in the range from 83.5 to 97.9% for birch and from 88.3 to 98.0% for pine, suggesting that pine wood was slightly more resistant toward pretreatments when compared to birch wood. Prolonging the pretreatment time together with increasing the temperature and the alkali charge clearly enhanced the material dissolution. The most important alkali-catalyzed degradation reactions responsible for the loss of polysaccharides included dissolution of non-degraded and partly degraded polysaccharides, deacetylation of acetyl groups in hemicelluloses, and primary peeling reaction (i.e., peeling reaction taking place in the polysaccharide chain reducing end units). Simultaneous formation of various hydroxy acids and the alkaline hydrolysis of glycosidic bonds in polysaccharide chains were followed by the formation of new alkali-labile reducing end groups amenable to the secondary peeling reaction (i.e., peeling reaction taking place on newly formed reducing end units, formed due to the cleavage of polysaccharide chains) [37–39]. In addition, minor dissolution and/or degradation of lignin from the feedstock as well as the removal of extractives took place.

3.2 ATR analyses

The ATR infrared spectra with corresponding band assignments recorded for the untreated birch and pine reference wood samples are shown in Fig. 1. Only some minor shifts in the spectra could be observed between these wood species. Characteristic absorption maxima generally assigned for wood polysaccharides (hemicelluloses and cellulose) could be observed at wavenumbers 1730, 1369, 1154, 1018, and 895 cm^{-1} for birch and at 1726, 1368, 1154, 1022, and 895 cm^{-1} for pine. Bands assigned for lignin aromatic structures could be determined having maxima at wavenumbers 1263 and 1229 cm^{-1} for birch and 1261 and 1232 cm^{-1} for pine (C=O and C–O groups in lignin) and those with maxima at wavenumbers 1603, 1507, and 1417 cm^{-1} for birch and 1603, 1508, and 1422 cm^{-1} for pine (caused by aromatic skeletal vibrations). These kinds of differences between the two investigated wood species could be expected, as their structures and chemical compositions (especially in terms of hemicelluloses and lignin) differ from each other [4].

Hardwood hemicelluloses are mainly composed of glucomannan and glucuronoxylan (referred later simply as xylan). Hardwood glucomannan (< 5% of the wood DS) has the same linear structure as softwood galactoglucomannan, but it is not substituted or acetylated [4]. Hardwood glucuronoxylan (between 20 and 30% of the wood dry mass) has the same linear structure as the softwood xylan, but it contains substantially fewer uronic acid substituents (two to three substituents per one xylan molecule) than softwood xylan. Moreover, the uronic acid substituents are not evenly distributed along the xylan chain. Hardwood xylan is partly acetylated at the C$_2$–OH and C$_3$–OH positions, with the acetyl group content varying from 8 to 17% of the total xylan, corresponding between 3.5 and 7.0 acetyl groups per 10 xylose units.

The corresponding softwood hemicelluloses are primarily composed of galactoglucomannans (glucomannan, from 15 to 20% of the wood DS), which is built of a linear backbone of $(1 \rightarrow 4)$-linked β-D-glucopyranose and β-D-mannopyranose units partly acetylated at C$_2$–OH and C$_3$–OH positions, and substituted by $(1 \rightarrow 6)$-linked α-D-galactopyranose units [4]. The other main softwood hemicellulose component arabinoglucuronoxylan (referred later as xylan, from 5 to
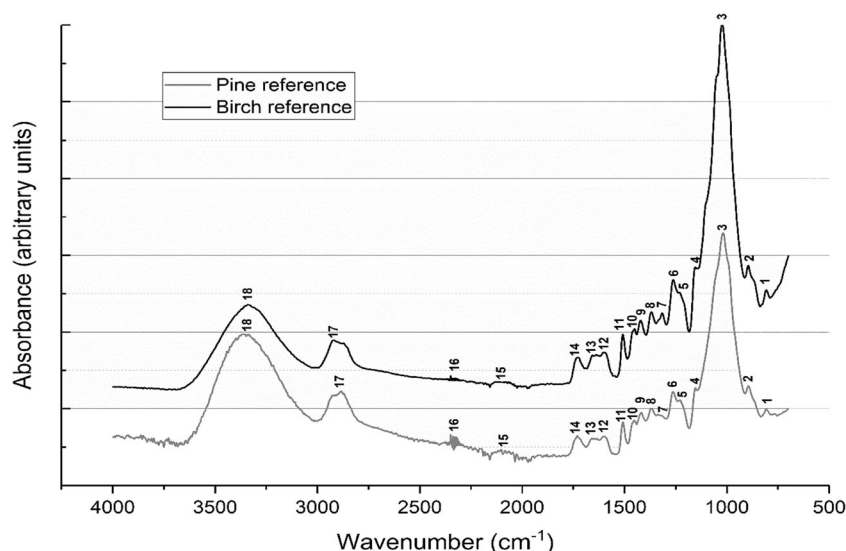
Fig. 1 ATR infrared spectra for untreated birch (black line) and pine (gray line) wood. Band assignments for the numbered peaks are as follows [26, 27, 30, 40, 41]: (1) 807 cm^{-1}: undefined (2) 895 cm^{-1}: CH out of plane glucose ring in cellulose and hemicelluloses, and for guaiacyl rings in lignin, COC, CCO, and CCH deformation stretching; (3) 1018– 1022 cm^{-1}: CO stretching in cellulose and lignin, CC, COH, and CH ring and side group vibrations; (4) 1154 cm^{-1}: COC stretching in pyranose rings and CO stretching in aliphatic groups, COC symmetric stretching, and OH plane deformation; (5) 1229–1232 cm^{-1}: COC stretching in phenol-ether bonds of lignin, CO stretching in syringyl rings, COC symmetric stretching, and OH plane deformation; (6) 1261– 1263 cm^{-1}: stretching of OCO and guaiacyl ring, CO stretching in lignin, and CO linkages in guaiacyl aromatic methoxyl groups; (7) 1315 cm^{-1}: undefined; (8) 1368–1369 cm^{-1}: aliphatic CH stretching in methyl and phenol OH, CH deformation in cellulose and hemicelluloses, in plane CH bending; (9) 1417–1422 cm^{-1}: aromatic skeletal vibrations combined with CH in plane deformation for lignin and cellulose; (10) 1451– 1453 cm^{-1}: CH$_2$ deformation stretching in lignin and xylan, CH deformation asymmetric in plane for lignin and hemicelluloses, HCH and OCH in plane bending vibration; (11) 1507–1508 cm^{-1}: aromatic skeletal stretching, C=C aromatic cycle, aromatic skeletal vibrations in guaiacyl rings; (12) 1603 cm^{-1}: C=C aromatic cycle, aromatic skeletal vibrations typical for syringyl units, and C=O stretching; (13) 1655– 1658 cm^{-1}: ab6sorbed OH and conjugated CO in lignin or cellulose, HOH, OH bending of absorbed water; (14) 1726–1730 cm^{-1}: C=O stretching in unconjugated ketone, carbonyl, and aliphatic groups (xylan), C=O vibration of esters, ketones, and aldehydes in hemicelluloses; (15) 2082–2101 cm^{-1}: undefined; (16) 2336– 2349 cm^{-1}: undefined; (17) 2883–2921 cm^{-1}: CH stretching in methyl and methylene groups, CH symmetrical stretching; and (18) 3338– 3359 cm^{-1}: OH stretching in hydroxyl groups

10% of the wood DS) is composed of linear $(1 \rightarrow 4)$-linked β-D-xylopyranose units substituted with $(1 \rightarrow 2)$-linked pyranoid 4-*O*-methyl-α-D-glucuronic acid and $(1 \rightarrow 3)$-linked α-L-arabinofuranose side groups (average molar ratios being 10:2:1.3 for xylose, uronic acid, and arabinose, respectively).

With regard to lignin, in hardwoods, the guaiacyl-syringyl-type lignin predominates, as its biosynthesis is based on the phenolic precursors *trans*-coniferyl and *trans*-sinapyl alcohols (in a rough ratio of 50:50). Softwood lignin is usually of guaiacyl-type, with structural elements mainly originating from *trans*-coniferyl alcohol (90%) with the remainder consisting mainly of *trans-p*-coumaryl alcohol.

The ATR infrared spectra presenting the effects caused by increasing pretreatment severity are shown in Fig. 2. In general, these spectra can be divided into three distinctive regions showing increased intensities caused by the pretreatments. The first wavenumber region from 2500 to 3750 cm^{-1} shows a clear increase in the intensities caused by OH stretching of hydroxyl groups and CH stretching, with both groups commonly associated to carbohydrate and lignin structures [26, 27, 30]. The increasing intensity caused by OH stretching of hydroxyl groups can be partly explained by the behavior of

carbohydrates under alkaline conditions; especially, amorphous hemicelluloses are degraded by alkali-catalyzed reactions (i.e., via primary peeling, alkaline hydrolysis, and secondary peeling), leading to the formation of new reducing end groups (i.e., hemiacetals) containing hydroxyl groups [39]. Moreover, new phenolic hydroxyl groups can be formed due to the cleavage of lignin bonds (especially β-aryl-ether structures) under alkaline conditions.

The second interesting wavenumber region ranging from 1100 to 1800 cm^{-1} contains several spectral peaks, which can be attributed to individual lignin (such as syringyl and guaiacyl precursors) and hemicellulose (mainly xylan) moieties [26, 27, 40, 41]. Within this region, the intensities of especially lignin-derived peaks were higher compared to the reference materials. This observation could be explained by the fact that under the pretreatment conditions applied, only a very small portion of the native lignin was degraded and dissolved. Therefore, the relative portion of lignin remaining in the wood increased.

The third region ranging from 800 to 1100 cm^{-1} can be explained mainly by the presence of carbohydrate components (cellulose and hemicelluloses) [26, 40, 41]. Due to the
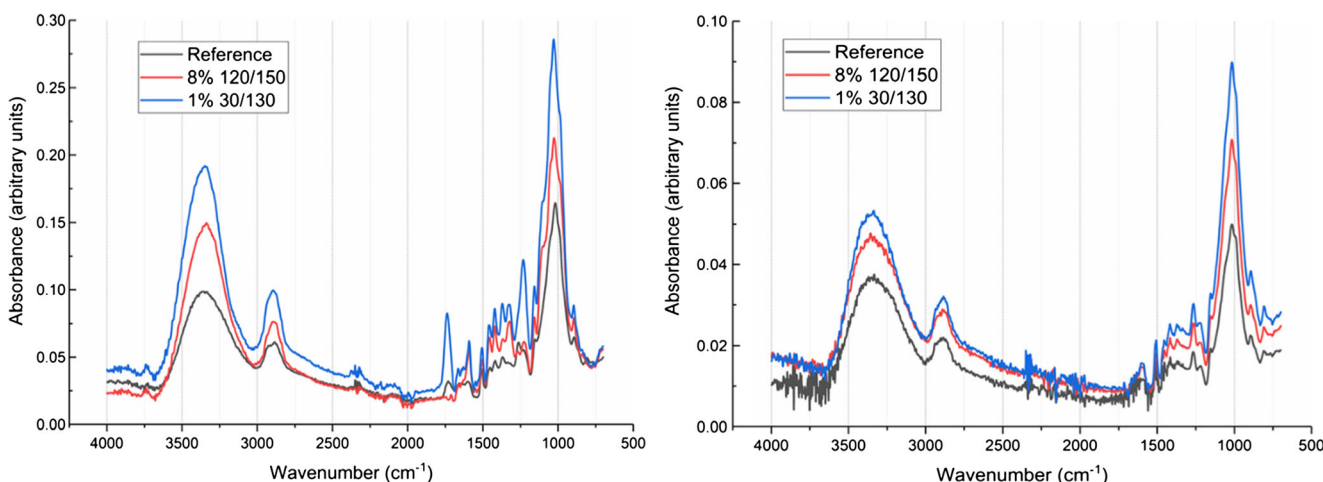
Fig. 2 ATR infrared spectra of birch (left) and pine (right) wood treated at varying pretreatment conditions (alkali charges as % and pretreatment time/temperature as min/°C)

highly crystalline nature and high degree of polymerization (when compared to hemicelluloses), cellulose was not significantly affected by applied pretreatment conditions but was enriched in the pretreated wood residues. In addition to the changes in the composition of the carbohydrate fraction, slight differences between the investigated wood samples can be explained by different composition of the lignin fraction. As mentioned above (Fig. 1), in hardwoods, the guaiacyl-syringyl-type lignin predominates, whereas softwood lignin is usually of guaiacyl-type. It is very likely that different lignin types also behave differently during the pretreatments.

ATR infrared spectra (wavenumber region from 700 to 1800 cm^{-1}) for birch and pine wood treated at varying pretreatment temperatures, times, and with 1 and 8% alkali charges are presented in Fig. 3. It could be concluded that prolonging the treatment time and increasing the treatment temperature did not cause any significant differences in the composition of the wood samples. However, increasing the
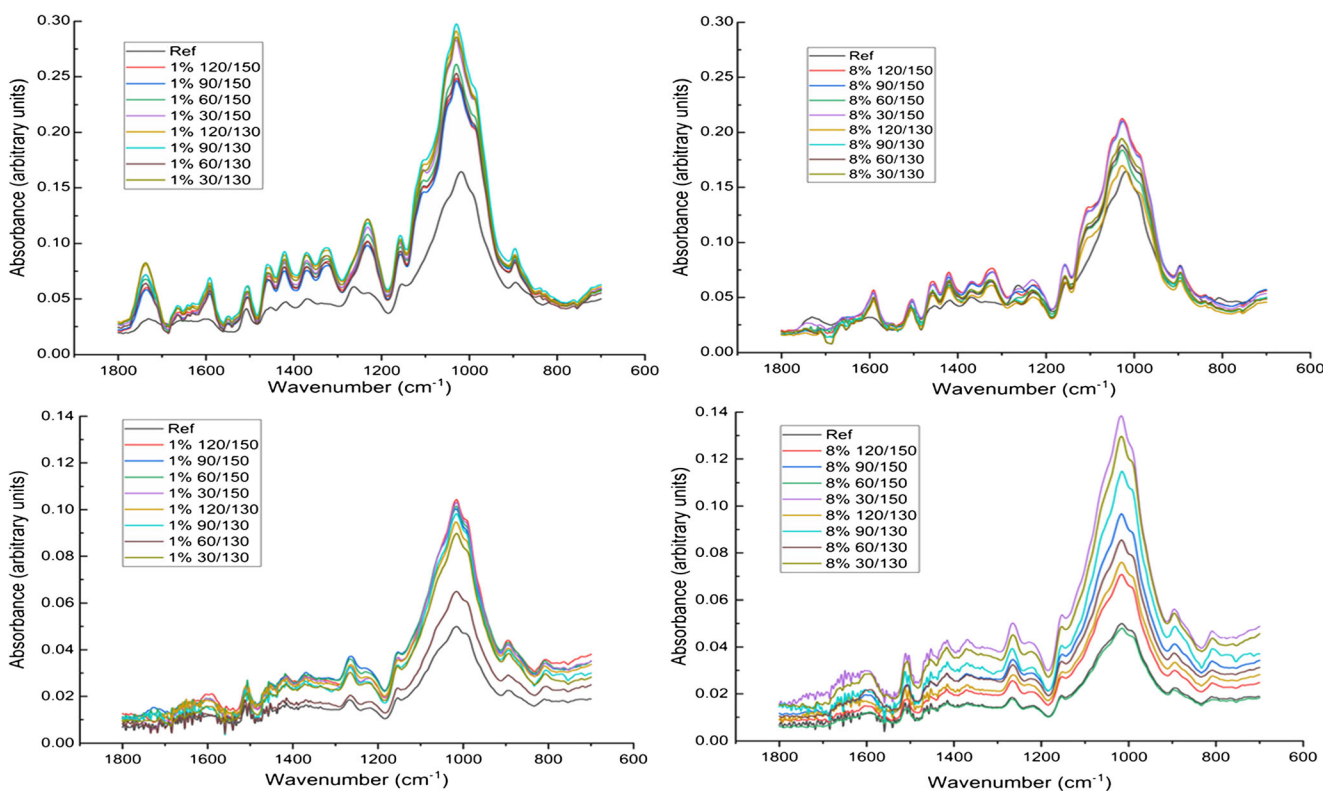

Fig. 3 ATR infrared spectra of birch (top) and pine (bottom) wood treated at varying pretreatment temperatures, times, and with alkali charges 1% (left) and 8% (right)
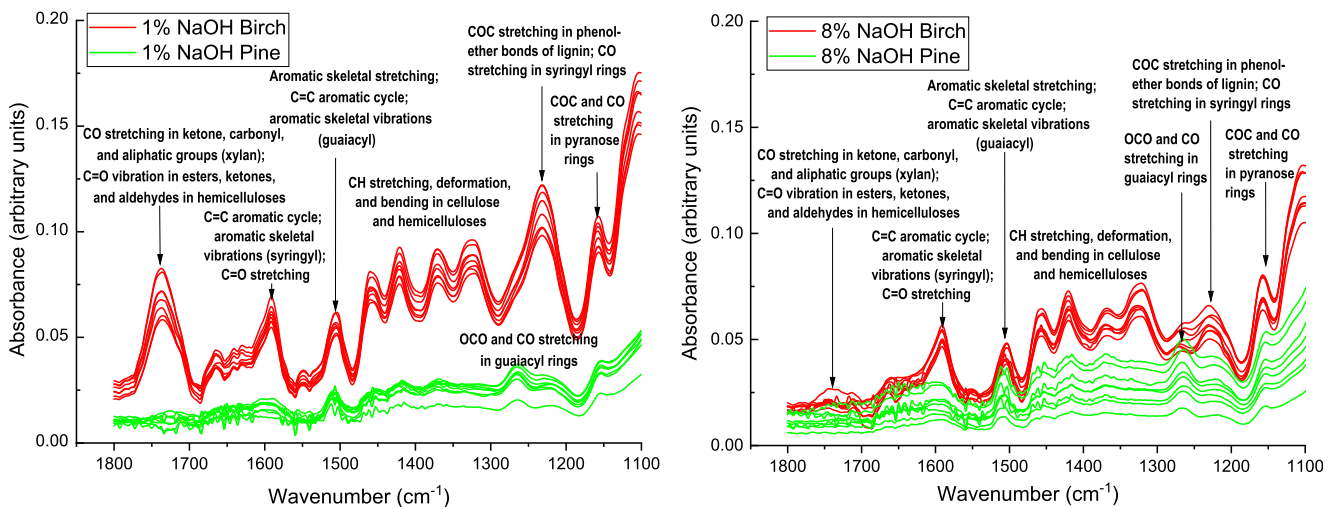
Fig. 4 ATR infrared spectra of the wavenumber region ranging from 1100 to 1800 cm^{-1} for birch (red) and pine (green) wood samples treated at varying pretreatment temperatures, times, and with different alkali charges 1% (left) and 8% (right)

alkali charge from 1 to 8% (on wood DS) clearly had an effect on the wood composition, especially on the presence of hemicelluloses.

ATR infrared spectra of the wavenumber region ranging from 1100 to 1800 cm^{-1} for the pretreated wood samples are presented in Fig. 4. Compositional differences between the two investigated wood species could be easily detected when the spectra from this wavenumber region were compared. In the region ranging from 1700 to 1780 cm^{-1}, the peak having

an absorption maximum at 1730 cm^{-1} was mainly caused by C=O transformations in unconjugated ketones, aldehydes, esters, carbonyls, and aliphatic groups found in hemicelluloses, especially in the hardwood xylan [26, 27, 40, 41]. Again, the effect of increased alkali charge on the content of birch xylan was clear, as this peak practically disappeared from the spectra recorded from those birch samples treated with the highest alkali solutions, suggesting an extensive dissolution of xylan during these harshest pretreatments. Additionally, the
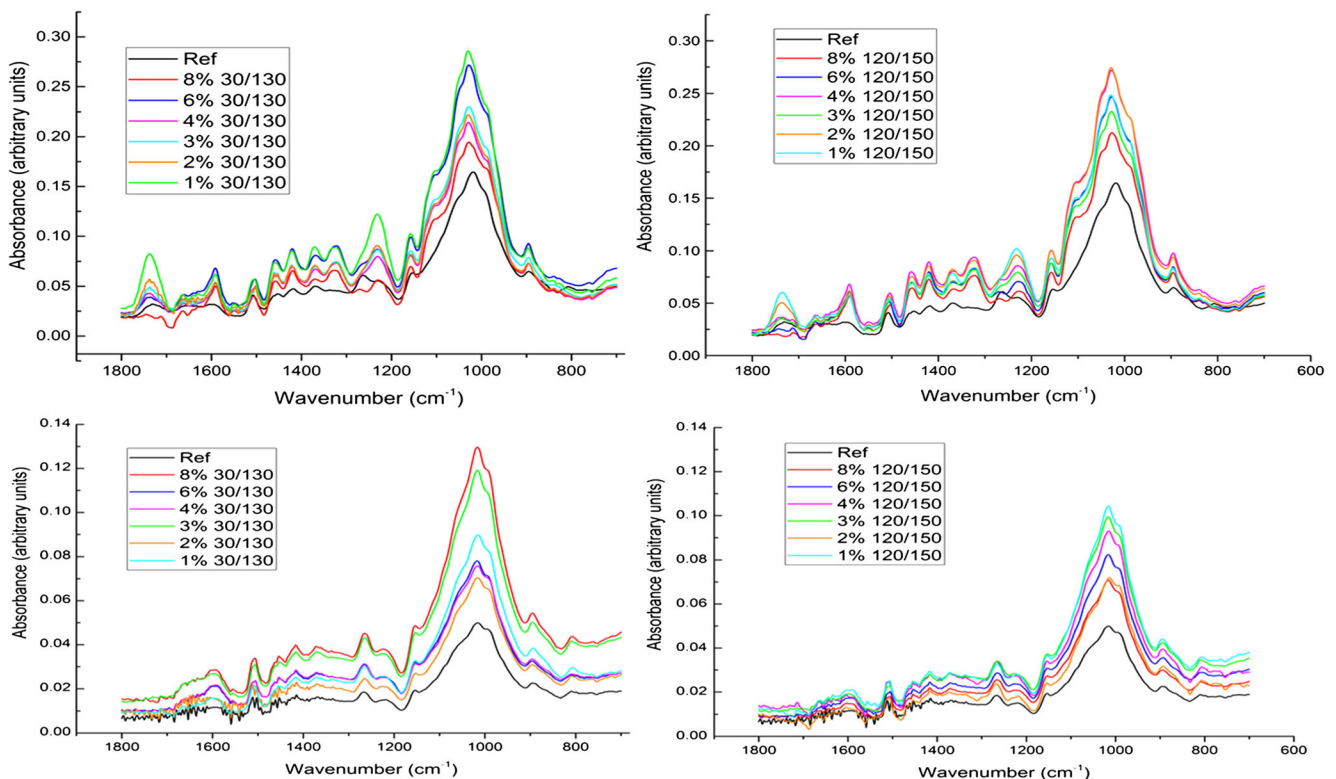

Fig. 5 ATR infrared spectra of birch (top) and pine (bottom) wood treated at varying alkali charges: 30 min at 130 °C (left) and 120 min at 150 °C

intensities of the peaks at the vicinity of wavenumbers 1370 and 1450 cm⁻¹ (mainly attributed to hemicelluloses-derived structures) [26, 40, 41] clearly decreased when the pretreatment conditions became harsher. The extensive removal of hemicelluloses, especially during harsh pretreatments, decreased intensities of the carbohydrate-related peaks.

The second main difference between the two investigated wood species could be traced to the presence of various species-specific lignin precursors in the wavenumber region ranging from 1150 to 1600 cm⁻¹ [24, 26, 27, 40, 41]. In birch samples, the guaiacyl-syringyl-type lignin predominated, originating from *trans*-coniferyl and *trans*-sinapyl alcohol (in an approximate 50:50 ratio) units. In softwoods, guaiacyl-type lignin predominated, with its structural, biosynthetic precursors being composed mainly of *trans*-coniferyl alcohol (90%), the remainder consisting of *trans*-p-coumaryl alcohol. In the spectra of birch samples, the peaks particularly denoted to syringyl rings showing COC stretching in the phenol-ether bonds of lignin, C=C aromatic cycle, aromatic skeletal vibrations typical for syringyl units, and C=O stretching accounted for the peaks at wavenumbers in the vicinity of 1230 and 1580 cm⁻¹ [26, 27, 40, 41]. Increasing the pretreatment severity caused a clear decrease in the relative intensities in ester structures at wavenumber 1730 cm⁻¹ and conjugated carbonyl groups at 1660 cm⁻¹, indicating the destruction of β-O-4 structures of lignin [42]. Furthermore, the cleavage of the ether linkages in lignin was observed from the clear decrease in intensities of the bands near 1230 and 1510 cm⁻¹ (attributed to syringyl and guaiacyl lignin structures, respectively). The reasons for different vulnerabilities of various lignin β-O-4 bonds toward alkaline pretreatments have also been studied [43]. These studies have shown that α-hydroxy groups of syringyl-type lignins are relatively more acidic when compared to guaiacyl-type lignin and that

syringyl type lignin nuclei are better leaving groups when compared to the corresponding guaiacyl nuclei in the β-O-4 bond cleavage. These factors result in the β-O-4 bond of syringyl lignin being more prone to the alkaline-induced cleavage than that of guaiacyl lignin. In pine samples, clear peaks located at wavenumbers near 1260 cm⁻¹ (stretching of OCO and CO groups in guaiacyl lignin) and 1510 cm⁻¹ (aromatic skeletal stretching, C=C aromatic cycle, and aromatic skeletal vibrations in guaiacyl rings) are commonly attributed to softwood guaiacyl lignin [26, 27, 40, 41]. In general, the effect of increased pretreatment severity caused smaller changes in pine than in corresponding birch samples, again suggesting a more resilient nature of softwood toward alkaline pretreatments.

ATR infrared spectra (wavenumber region from 700 to 1800 cm⁻¹) for birch and pine wood treated for 30 min at 130 °C and for 120 min at 150 °C with varying alkali charges are presented in Fig. 5. Also in this case, when the spectra recorded from differently treated wood samples were compared to each other, it could be concluded that prolonging the treatment time and increasing the treatment temperature did not cause such significant differences in the composition of the wood samples as were caused by increasing the alkali charge. Increasing the alkali charge from 1 to 8% (on wood DS) clearly had an effect on the wood composition, especially on the presence of hemicelluloses. As mentioned above, especially birch xylan was found to be vulnerable to alkaline treatments, and significant degradation of its structure was evident.

ATR infrared spectra of the wavenumber region ranging from 1100 to 1800 cm⁻¹ for the wood samples treated for 30 min at 130 °C and for 120 min at 150 °C together with varying alkali charges are presented in Fig. 6. Compositional differences between the two investigated wood species were
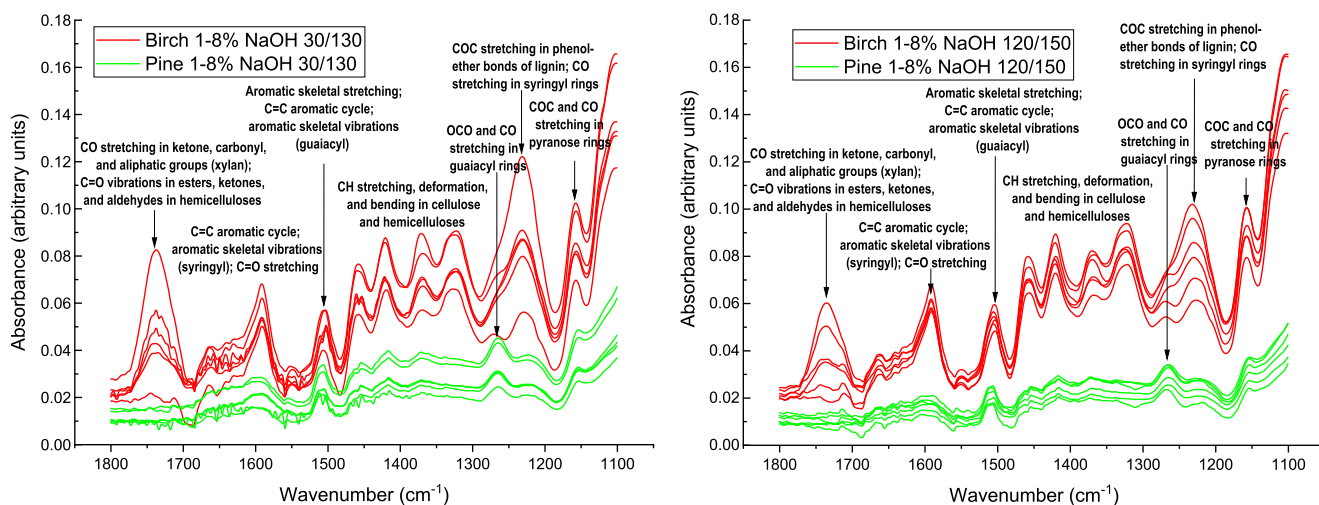

Fig. 6 ATR infrared spectra of the wavenumber region ranging from 1100 to 1800 cm⁻¹ for birch (red) and pine (green) wood samples treated for 30 min at 130 °C (left) and for 120 min at 150 °C (right) and with varying alkali charges

again easily detected when the spectral data from this wavenumber region were compared to each other. Additionally, investigating this specific wavenumber region containing the main part of information about the structure and behavior of lignin and hemicelluloses present in wood revealed the dominating effect of applied alkali charge on the degradation and dissolution of wood polymers. Especially evident changes in the wood structure could be observed in those wavenumber regions containing hemicelluloses (from 1700 to 1800 cm^{-1} originating mainly from hardwood xylan) and lignin (from 1550 to 1600 cm^{-1} originating from hardwood syringyl groups)-derived peaks. The effects of increased alkali additions together with increased harshness of thermal conditions clearly changed the chemical composition of the wood and the relative content of individual wood components were changed during the course of the pretreatments. In addition, the resilient nature of pine wood against mild alkaline pretreatments compared to the corresponding birch samples was confirmed. Much less changes in FTIR spectra could be observed for treated pine samples than for corresponding birch samples treated under the same pretreatment conditions.

4 Conclusions

Effects of alkaline pretreatments on chemical composition of hardwood (silver/white birch) and softwood (Scots pine) were investigated by attenuated total reflectance (ATR) infrared (IR) spectroscopy. Spectral data recorded from pretreated materials were compared to those from untreated reference materials to evaluate how simply and quickly this spectroscopy method could identify the phenomena taking place during the treatments. Interpretation of spectral data was supported by utilizing previously obtained chemical and literature data on the main lignin- and carbohydrates-related phenomena taking place during alkaline degradation of wood polymers. Results clearly indicated that this spectral method could detect several fundamental changes caused by pretreatments. This approach enabled the detailed description of differences between the treated wood species both in terms of chemical composition and behavior during the pretreatments. Likewise, various chemical phenomena, such as formation of different lignin and carbohydrate moieties under varying pretreatment conditions (i.e., temperature, time, and alkali charge) and dissolution of various structural wood components (mainly hardwood originated xylan and syringyl groups-containing lignin), could be explained by comparing the obtained spectral data with those from literature references and previous studies on materials dissolved during alkaline pretreatments. It could be determined that especially hardwood hemicelluloses and lignin were prone for chemical changes and dissolution during the alkaline pretreatments. In general, the changes in the structure and chemical composition of the softwood were found to

be relatively small, thus indicating more resilient nature of softwood hemicelluloses and lignin toward the mild alkaline pretreatments applied during this study when compared to corresponding hardwood counterparts. In addition, cellulose was found to be very resilient against the applied treatment conditions, thus confirming the fact that these kinds of pretreatments have only very limited effect on the cellulosic fiber. For this reason, these kinds of pretreatments can be considered promising alternatives for manufacturing especially hemicelluloses- and lignin-derived bioproducts from these common Nordic pulpwoods.

Publisher's Note Springer Nature remains neutral with regard to jurisdictional claims in published maps and institutional affiliations.

References

1. Hardy J (2004) Green chemistry and sustainability. In: Stevens CV, Verhé R (eds) Renewable bioresources—scope and modification for non-food applications. John Wiley & Sons Ltd, Chichester, pp 1–29

2. Kamm B, Kamm M, Gruber PR, Kromus S (2006) Biorefinery systems—an overview. In: Kamm B, Kamm M, Gruber PR, Kromus S (eds) Biorefineries—industrial processes and products, Status Quo and Future Directions. Wiley-VCH Verlag GmbH & Co. KGaA, Weinheim, pp 3–40

3. van Santen RA (2007) Renewable catalytic technologies—a perspective. In: Centi G, van Santen RA (eds) Catalysis for renewables—from feedstock to energy production. Wiley-VCH Verlag GmbH & Co. KGaA, Weinheim, pp 1–19

4. Alén R (2011) Principles of biorefining. In: Alén R (ed) Biorefining of Forest Resources Paper Engineers' Association, Helsinki, pp 18–114

5. Goldstein IS (1981) Organic chemicals from biomass. CRC press, Boca Raton

6. Sinsky AJ (1983) Organic chemicals from biomass: an overview. In: Wise DL (ed) Organic chemicals from biomass. Benjamin/Cummins Publishing Company, pp 1–67

7. Mateos-Espejel E, Moshkelani M, Keshtkar M, Paris J (2011) Sustainability of the green integrated forest biorefinery: question of energy. J Sci Technol For Prod Proc 1:55–61

8. van Heiningen A (2006) Converting a kraft pulp mill into an integrated forest biorefinery. Pulp Paper Can 107:38–43

9. Baijpai P (2012) Integrated forest biorefinery. In: Baijpai P (ed) Biotechnology for pulp and paper processing. Springer, New York, pp 375–402

10. Moshkelani M, Marinova M, Perrier M, Paris J (2013) The forest biorefinery and its implementation in the pulp and paper industry: energy overview. Appl Therm Eng 50:1427–1436

11. Ragauskas AJ, Nagy M, Kim DH, Eckert CA, Hallett JP, Liotta CL (2006) From wood to fuels—integrating biofuels and pulp production. Ind Biotechnol 2:55–65

12. Hämäläinen S, Näyhä A, Pesonen H-L (2011) Forest biorefineries—a business opportunity for the Finnish forest cluster. J Clean Prod 19:1884–1891

13. Carvalheiro F, Duarte LC, Gírio FM (2008) Hemicellulose biorefineries: a review on biomass pretreatments. J Sci Ind Res 67:849–864

14. von Weymarn N (2011) The sugar platform in the wood biorefinery. In: Proceedings of the 3rd Nordic wood and biorefinery conference (NWBC), Stockholm, Sweden: march, vol 22-24, p 138

15. Lehto JT, Alén RJ (2015) Chemical pretreatments of wood chips prior to alkaline pulping—a review of pretreatment alternatives, chemical aspects of the resulting liquors. and pulping outcomes BioResources 10:8604–8656

16. Chirat C, Lachenal D, Sanglard M (2012) Extraction of xylans from hardwood chips prior to kraft cooking. Process Biochem 47:381–385

17. Yoon S-H, Tunc MS, van Heiningen A (2011) Near-neutral pre-extraction of hemicelluloses and subsequent kraft pulping of southern mixed hardwoods. TAPPI J 10:7–15

18. Luo J, Genco JM, Zou H (2012) Extraction of hardwood biomass using dilute alkali. TAPPI J 11:19–27

19. Walton SL, Hutto D, Genco JM, van Walsum GP, van Heiningen ARP (2010) Pre-extraction of hemicelluloses from hardwood chips using an alkaline wood pulping solution followed by kraft pulping of the extracted wood chips. Ind Eng Chem Res 49:12638–12645

20. Yoon SH, van Heiningen A (2010) Green liquor extraction of hemicelluloses from southern pine in an integrated forest biorefinery. J Ind Eng Chem 16:74–80

21. Jun A, Tschirner UW, Tauer Z (2012) Hemicellulose extraction from aspen chips prior to kraft pulping utilizing kraft white liquor. Biomass Bioenergy 37:229–236

22. Hendriks ATWM, Zeeman G (2009) Pretreatments to enhance the digestibility of lignocellulosic biomass. Bioresour Technol 100:10–18

23. Huang F, Ragauskas A (2013) Integration of hemicellulose pre-extraction in the bleach-grade pulp production process. TAPPI J: 1255–1261

24. Martin-Sampedro R, Eugenio ME, Moreno JA, Revilla E, Villar JC (2014) Integration of a kraft pulping mill into a forest biorefinery: pre-extraction of hemicellulose by steam explosion versus steam treatment. Bioresour Technol 153:236–244

25. Tjeerdsma BF, Militz H (2005) Chemical changes in hydrothermal treated wood: FTIR analysis of combined hydrothermal and dry heat-treated wood. Holz Roh Werkst 63:102–111

26. Huang A, Zhou Q, Liu J, Fei B, Sun S (2008) Distinction of three wood species by Fourier transform infrared spectroscopy and two-dimensional correlation IR spectroscopy. J Molec Struct 883-884: 160–166

27. Vartanian E, Barres O, Roque C (2015) FTIR spectroscopy of woods: a new approach to study the weathering of the carving face of a sculpture. Spectrochim Acta Part A 136:1255–1259

28. Mehrotra R, Singh P, Kandpal H (2010) Near infrared spectroscopic investigation of the thermal degradation of wood. Thermoch Acta 507-508:60–65

29. Popescu C-M, Popescu M-C (2013) A near infrared spectroscopic study of the structural modifications of lime (Tilia cordata Mill.) wood during hydro-thermal treatment. Spectrochim Acta Part A 115:227–233

30. Chen Z, Hu TQ, Jang HF, Grant E (2015) Modification of xylan in alkaline treated bleached hardwood kraft pulps as classified by attenuated total-internal-reflection (ATR) FTIR spectroscopy. Carbohydr Polym 127:418–426

31. Pizzo B, Pecoraro E, Alves A, Macchioni N, Rodrigues JC (2015) Quantitative evaluation by attenuated total reflectance infrared (ATR-FTIR) spectroscopy of the chemical composition of decayed wood preserved in waterlogged conditions. Talanta 131:14–20

32. SCAN-CM 40:94 (1994) Wood chips for pulp production—size distribution, Scandinavian Pulp, Paper and Board Testing Committee, Stockholm

33. TAPPI T280 pm-997 (1999) Acetone extractives of wood and pulp, TAPPI Press, Atlanta

34. TAPPI T222 om-98 (1998) Acid insoluble lignin in wood and pulp TAPPI Press, Atlanta

35. TAPPI T250 um-00 (2000) Acid-soluble lignin in wood and pulp, TAPPI Press, Atlanta

36. Swan B (1965) Isolation of acid-soluble lignin from the Klason lignin determination. Svensk Papperstidn 68:791–795

37. Lehto J, Alén R (2013) Alkaline pre-treatment of hardwood chips prior to delignification. J Wood Chem Technol 33:77–91

38. Lehto J, Alén R (2015) Alkaline pre-treatment of softwood chips prior to delignification. J Wood Chem Technol 35:146–155

39. Alén R (2000) Basic chemistry of wood delignification. In: Stenius P (ed) Forest Products Chemistry Fapet Oy, Helsinki, pp 58–104

40. Traoré M, Kaal J, Cortizas AM (2016) Application of FTIR spectroscopy to the characterization of archeological wood. Spectrochim Acta Part A 153:63–70

41. Fan M, Dai D, Huang B (2012) Fourier transform infrared spectroscopy for natural fibres. In: Salih S (ed) Fourier transform—materials analysis. InTech, Shanghai, pp 45–68

42. Wang P, Fu Y, Shao Z, Zhang F, Qin M (2016) Structural changes to aspen wood lignin during autohydrolysis pretreatment. BioResources 11:4086–4103

43. Shimizu S, Akiyama T, Yokoyama T, Matsumoto Y (2017) Chemical factors underlying the more rapid β-O-4 bond cleavage of syringyl than guaiacyl lignin under alkaline delignification conditions. J Wood Chem Technol 37:451–466